Journal of Cerebral Blood Flow & Metabolism (2014) 34, 1434–1439

www.jcbfm.com

OPEN

RAPID COMMUNICATION

Adequacy of a compartment model for $CMRO_2$ quantitation using ^{15}O-labeled oxygen and PET: a clearance measurement of ^{15}O-radioactivity following intracarotid bolus injection of ^{15}O-labeled oxyhemoglobin on *Macaca fascicularis*

Hidehiro Iida[1], Satoshi Iguchi[1], Noboru Teramoto[1], Kazuhiro Koshino[1], Tsutomu Zeniya[1], Akihide Yamamoto[1], Nobuyuki Kudomi[1,2], Tetsuaki Moriguchi[1], Yuki Hori[1], Junichiro Enmi[1], Hidekazu Kawashima[1], Nadim Joni Shah[3] and Jyoji Nakagawara[4]

We aimed at evaluating the adequacy of the commonly employed compartmental model for quantitation of cerebral metabolic rate of oxygen ($CMRO_2$) using ^{15}O-labeled oxygen ($^{15}O_2$) and positron emission tomography (PET). Sequential PET imaging was carried out on monkeys following slow bolus injection of blood samples containing $^{15}O_2$–oxyhemoglobin ($^{15}O_2$–Hb), ^{15}O-labeled water ($H_2^{15}O$), and $C^{15}O$-labeled hemoglobin ($C^{15}O$–Hb) into the internal carotid artery (ICA). Clearance slopes were assessed in the middle cerebral artery territory of the injected hemisphere. The time–activity curves were bi-exponential for both $^{15}O_2$–Hb and $H_2^{15}O$. Single exponential fitting to the early (5 to 40 seconds) and late (80 to 240 seconds) periods after the peak was performed and the $^{15}O_2$–Hb and $H_2^{15}O$ results were compared. It was found that a significant difference between the clearance rates of the $^{15}O_2$–Hb and $H_2^{15}O$ injections is unlikely, which supports the mathematical model that is widely used to describe the kinetics of $^{15}O_2$–Hb and $H_2^{15}O$ in cerebral tissues and is the basis of recent approaches to simultaneously assess $CMRO_2$ and cerebral blood flow in a single PET session. However, it should be noted that more data are necessary to unequivocally confirm the result.

Journal of Cerebral Blood Flow & Metabolism (2014) **34,** 1434–1439; doi:10.1038/jcbfm.2014.118; published online 9 July 2014

Keywords: CBF; $CMRO_2$; compartment model; ^{15}O-labeled hemoglobin; PET

INTRODUCTION

Use of ^{15}O-labeled molecular oxygen ($^{15}O_2$) is an ideal molecule for tracing the kinetics of oxygen *in vivo*, and allows quantitative assessment of regional cerebral metabolic rate of oxygen ($CMRO_2$) *in vivo*. Several mathematical approaches have been developed to estimate functional images of $CMRO_2$ from positron emission tomography (PET) images acquired following continuous or short-period inhalation of $^{15}O_2$, together with additional assessments of regional cerebral blood flow (CBF) and regional cerebral blood volume. The calculation process is based on a model, in which the fraction of labeled oxygen that diffuses into brain tissue is rapidly reduced by cytochrome oxidase of the mitochondrial electron transfer system, immediately converted to ^{15}O-labeled water ($H_2^{15}O$), and washed out according to CBF. It has therefore been assumed that the back diffusion of $^{15}O_2$ is negligibly small (Figure 1). It is also assumed that there is negligible amount of retention of $^{15}O_2$ in the cerebral tissue (Figure 1). These enable that the clearance after the $^{15}O_2$ transport from tissue to capillary bed can be compensated using CBF information obtained from an independent PET scan with $H_2^{15}O$. The practical procedures to estimate $CMRO_2$ from a series of PET scanning such as the steady-state technique[1–3], the three-step autoradiography[4], and single-step approaches[5–7] are straightforward and have been successfully applied to a number of clinical studies.

The clearance of ^{15}O-radioactivity after the intracarotid bolus injection of ^{15}O-labeled oxygen ($^{15}O_2$) in the form of oxyhemoglobin has been first measured using a single gamma photon detector in humans. Slopes were claimed to be consistent between $^{15}O_2$–oxyhemoglobin ($^{15}O_2$–Hb) and $H_2^{15}O$,[8,9] but a significant level of background due to the limited collimation of the detector was a limitation. Thus, another experiment was carried out recently by Seki *et al*[10] using a beta ray-sensitive plastic scintillator directly attached to the surface of rat brain. They demonstrated that the clearance after the internal carotid bolus injection of $^{15}O_2$–Hb was considerably faster than that of $H_2^{15}O$, suggesting the presence of back diffusion of $^{15}O_2$ from brain tissue in addition to the back flux of $H_2^{15}O$. However, there could be several technical limitations, including the insufficient collimation of their detector system, and the relatively large volume of administrated $^{15}O_2$–Hb containing blood samples. It is, therefore, still an important issue to confirm whether or not the clearance slope of ^{15}O-radioactivity after the internal carotid artery (ICA) bolus injection of $^{15}O_2$–Hb agrees with that of $H_2^{15}O$–saline.

In the present study, we intended to reevaluate the adequacy of the compartmental model commonly employed for $^{15}O_2$-inhalation PET studies using a bigger animal. Clearance of the radioactivity concentration in local brain regions were quantitatively assessed on the nonhuman primate of *Macaca fascicularis*

[1]Department of Investigative Radiology, National Cerebral and Cardiovascular Center Research Institute, Suita City, Osaka, Japan; [2]Department of Medical Physics, Faculty of Medicine, Kagawa University, Kitagun, Kagawa, Japan; [3]Institute of Neuroscience and Medicine 4, Medical Imaging Physics, Forschungszentrum Jülich GmbH, Jülich, Germany and [4]Integrative Stroke Imaging Center, Department of Neurosurgery, National Cerebral and Cardiovascular Center, Suit City, Osaka, Japan. Correspondence: Dr H Iida, Department of Investigative Radiology, National Cerebral and Cardiovascular Center Research Institute, 5-7-1, Fujishirodai, Suita City, Osaka 565-8565, Japan.
E-mail: iida@ri.ncvc.go.jp

The present work was supported by a Grant from the Ministry of Health, Labor and Welfare, Japan.
Received 29 June 2012; revised 4 June 2014; accepted 4 June 2014; published online 9 July 2014

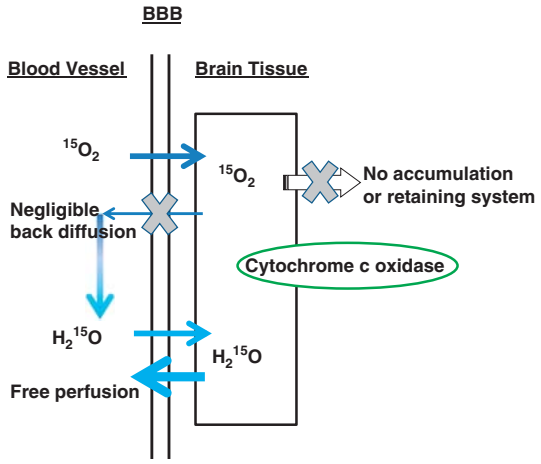

Figure 1. Tracer model commonly employed for describing radioactivity kinetics after $^{15}O_2$–hemoglobin ($^{15}O_2$–Hb) injection. The model consists of a vascular compartment, a non-metabolized oxygen compartment, and a metabolized water compartment. Negligible amount of back diffusion in the form of ^{15}O-labeled oxygen ($^{15}O_2$) is attributed to the short life time of molecular oxygen in the cerebral tissue. No accumulation or retaining system exist for $^{15}O_2$ oxygen, neither for ^{15}O-labeled water ($H_2^{15}O$). BBB, blood–brain barrier.

after the ICA injection of $^{15}O_2$–Hb and $H_2^{15}O$, from sequentially acquired tomographic images using an advanced PET scanner. We then evaluated whether or not we are able to identify the significant difference in the clearance slopes between the $^{15}O_2$–Hb and $H_2^{15}O$ samples.

MATERIALS AND METHODS

Subjects

Two monkeys (*M. fascicularris*) were selected for a series of dynamic PET scanning, from a group prepared for another project that investigated outcome of the revascularization trial in acute stroke model. Both are healthy normal male, age of 3 and 4 years old, and the body weight of 7.5 and 7.0 kg, respectively. In total, three sessions of PET studies were carried out, namely once on one monkey and twice on another monkey. Animals were maintained and handled in accordance with guidelines for animal research on Human Care and Use of Laboratory Animals (Rockville, National Institute of Health/Office for Protection from Research Risks, 1996). The study protocol was approved by the Sub-committee for Laboratory Animal Welfare, National Cerebral and Cardiovascular Center Research Institute, Osaka, Japan.

Animal Preparation

Anesthesia was induced with ketamine (10 mg/kg, intramuscularly) and maintained by intravenous propofol (4 mg/kg per hour) and vecuronium (0.05 mg/kg per hour) during the experiment. Animals were intubated and their respiration was controlled by an anesthetic ventilator (Cato; Drager, Lubeck, Germany) providing a gas mixture of 24% O_2 and 76% N_2[6,7,11]. A catheter was inserted into the ICA for intracarotid bolus injection of $^{15}O_2$–Hb, $H_2^{15}O$, and C^{15}O–hemoglobin (C^{15}O–Hb). A catheter was also inserted into the femoral artery for monitoring the blood pressure, heart rate, O_2 content, and the partial pressures of carbon dioxide level in arterial blood. Additional catheter was placed to the anterior tibial vein, and was utilized for infusing the anesthetic agents.

Preparation of $^{15}O_2$–Hemoglobin, C^{15}O–Hemoglobin, and $H_2^{15}O$–Saline

^{15}O-radioactivity was produced by the ^{14}N(d,n)^{15}O nuclear reaction with a 0.5% O_2/N_2 gas target using a CYPRYS-HM18 cyclotron (Sumitomo Heavy Industry, Tokyo, Japan). The bombarded target gas including the produced $^{15}O_2$ was transported to an in-house synthesizer system to achieve high radiochemical purity for each $^{15}O_2$ and C^{15}O gases. The $^{15}O_2$–Hb and C^{15}O–Hb were prepared using the labeling system developed by Magata *et al*[12]. Briefly, a part of an infusion line kit (Terumo Corporation, Tokyo, Japan) and an artificial lung 18 cm in length (Senko Medical Instrument Manufacturing, Tokyo, Japan) were connected using silicone tubing to make a closed blood circulating system (see Figure 2). Venous blood collected from each monkey was infused into the system and was circulated by a peristaltic pump at a flow rate of 100 mL/minute, with the introduction of $^{15}O_2$ and/or C^{15}O gases at ~7,000 MBq/minute/500 mL into the artificial lung for 5 to 15 minutes, producing the $^{15}O_2$–Hb and C^{15}O–Hb samples of ~60 MBq/mL. A coincidence detector block containing a pair of GSO scintillator[13] was implemented to monitor the radioactivity in the circulating blood. The $^{15}O_2$–Hb and C^{15}O–Hb samples were adjusted to contain radioactivity of ~17 MBq in 0.4 mL at the time of injection into the ICA.

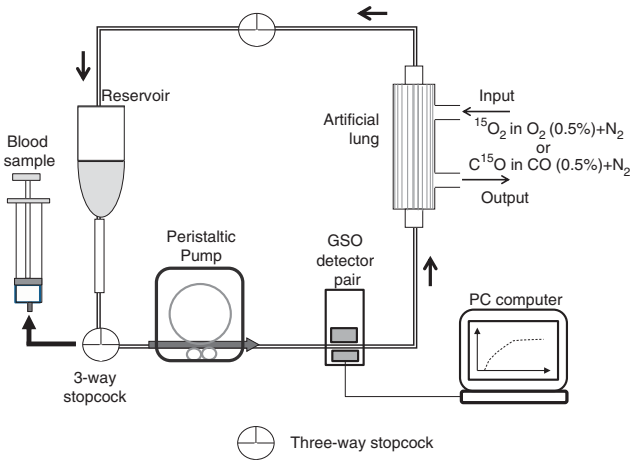

Figure 2. Schematic diagram of a system to generate the blood samples containing $^{15}O_2$–hemoglobin ($^{15}O_2$–Hb) and C^{15}O–hemoglobin (C^{15}O–Hb). The system is the same as the one described in Magata *et al*.[12] An additional radioactivity detector was placed to monitor the radioactivity in the circulating blood sample.

The $^{15}O_2$ gas was also transferred to $H_2^{15}O$ using a radioactive water generator[14] to produce the injectable saline containing $H_2^{15}O$. The $H_2^{15}O$–saline was diluted by the arterial blood of more than eight times volume, and had radioactivity of ~20 MBq in 0.4 mL at the time of bolus injection into the ICA.

Positron Emission Tomography Experiments

The PET scanner was ECAT HR, Siemens-CTI (Knoxville, TN, USA) containing BGO scintillator blocks, which can acquire the data either in two-dimensional or in three-dimensional modes. The scanner provides tomographic images for 47 slices for an imaging field of view of 55 cm in diameter and 15 cm in axial length. The intrinsic spatial resolution was 5.8 mm in full width at half maximum at the center of the field of view. Observed spatial resolution after applying the three-dimensional Gaussian post filter, the observed spatial resolution was ~10 mm.

At least 1 hour after the end of the preparation for catheter, we confirmed that the heart rate, the arterial blood pressure, and the arterial partial pressures of carbon dioxide and oxygen can be maintained constant, a series of PET scans were initiated. A 900-second transmission scan was first carried out using a rotating ^{68}Ge-^{68}Ga rod source for the attenuation correction. Each of $^{15}O_2$–Hb (~17 MBq), $H_2^{15}O$–saline (20 MBq), and C^{15}O–Hb (17 MBq) samples of 0.4 mL were injected in 3 to 4 seconds into either the right or the left ICA. Three sets of list mode acquisition were carried out in two-dimensional mode for 5.5 minutes, for each injection. The order was the same in all three experiments, because this is the easiest protocol in our radio synthesizing system.

Data Analysis

The list mode data were sorted to produce dynamic sinogram for each scan, with frame durations of 30 times 1 second, 15 times 2 seconds, 12 times 5 seconds, and 18 times 10 seconds, in total 5 minutes. Images were then reconstructed using a filtered back projection technique, including

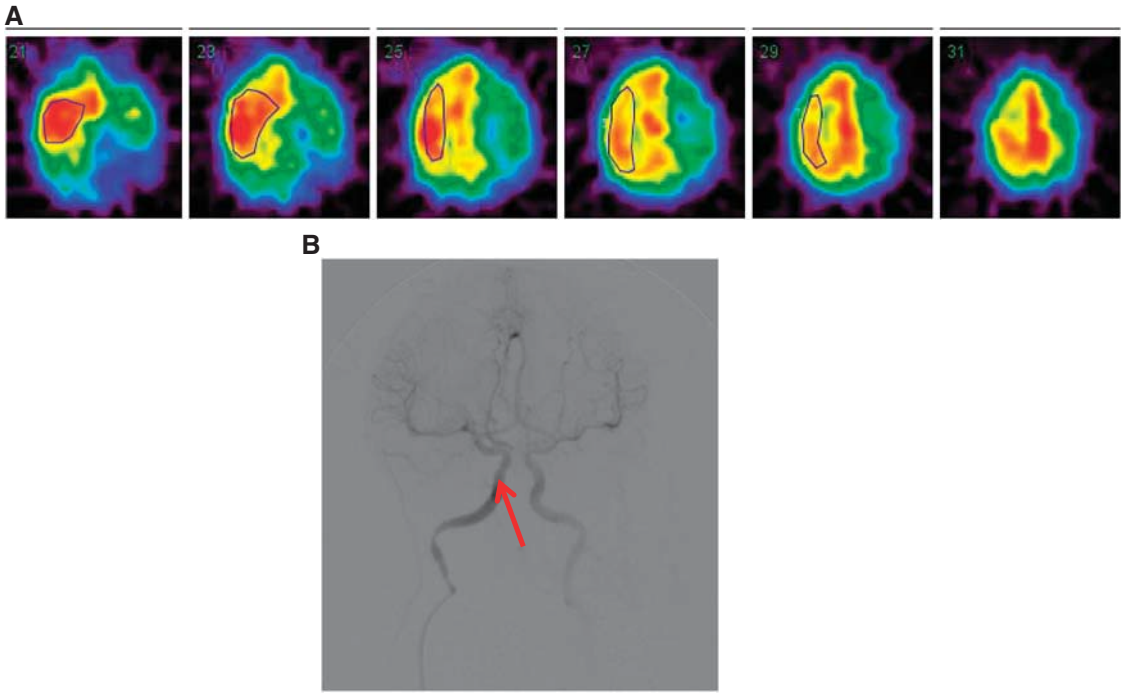

Figure 3. (**A**) Regions of interest (ROIs) placed on each at the monkey experiments. Five ROIs were selected on the accumulated positron emission tomography (PET) images over the initial 50 seconds after the peak, on the middle cerebral artery territory of the injected hemisphere at different slice levels. In the PET images, radioactivity from the contralateral to the injected hemisphere was attributed to the collateral circulation though the Willis Ring. (**B**) An example image of angiography carried out prior to the carotid artery injection of ^{15}O-labeled samples.

corrections for dead time, the radioactive decay, detectors normalization, attenuation, and scatter, using the vendor software programs. Dynamic PET images following the intracarotid injection of $H_2^{15}O$ were added over the initial 50 seconds after the peak of the head curve. Five regions of interest were defined on this image for each experiment (see Figure 3), in the middle cerebral artery territory of the injected hemisphere on different slice levels, providing five sets of clearance curves for each injection. Angiography was carried out in order to confirm the location for the coronary arterial injection. It was also monitored that 0.4 mL sample does not interfere the natural cerebral circulation. Each clearance curve after the $^{15}O_2$–Hb and $H_2^{15}O$–saline injection was fitted to a single exponential function during the first 5 to 40 seconds (early), and 80 to 240 seconds (late) periods after the peak. Mean and s.d. were calculated for slope values for each of the early and late phases, and also for both $^{15}O_2$–Hb and $H_2^{15}O$–saline for each experiment. Significant difference in the slope parameters was identified between $^{15}O_2$–Hb and $H_2^{15}O$–saline, using a Student's *t*-test (paired one-tail, one-tail). Residues of the single exponential fit from the measured data were calculated, and the presence of the significant correlation was tested on the semi-logarithmic domain using Pearson's test. $P < 0.05$ was considered statistically significant throughout the study.

RESULTS

Positron emission tomography scans were successfully carried out on all animals for all injections, with the variation of partial pressures of carbon dioxide < 1 mm Hg, the systolic/diastolic blood pressure < 4 mm Hg, the heart rate $< 5\%$ throughout the study at each experiment. Typical coincidence counting rate of the whole PET gantry was ~ 35, 60, and 30 kcps at peak, corresponding to the $^{15}O_2$–Hb, $H_2^{15}O$–saline, and $C^{15}O$–Hb injections, respectively. The dead time counting loss was $< 5\%$ at peak in all scans.

Figure 4 shows a typical example of the clearance curves obtained following the $^{15}O_2$–Hb, $H_2^{15}O$–saline, and $C^{15}O$–Hb sample injections into one of the experiments in middle cerebral artery territory of the central slice. The clearance is rapid after the $C^{15}O$–Hb sample injection, while they consisted of slower slopes with $^{15}O_2$–Hb and $H_2^{15}O$–saline injections. It can be seen that the

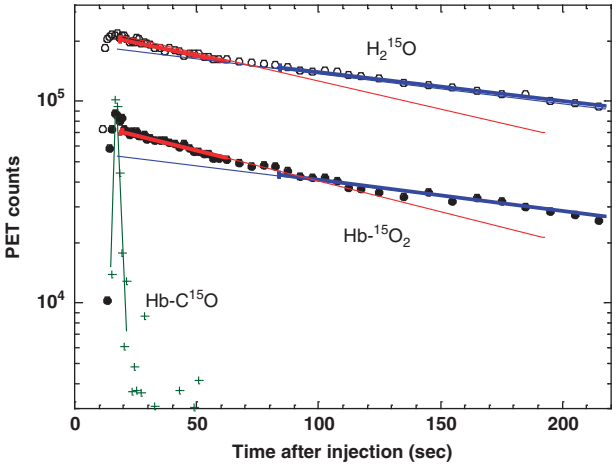

Figure 4. Typical results from the clearance measurement, with results of fitting by single exponential function for the early (5 to 40 seconds) and late (80 to 240 seconds) periods, indicated with blue and red lines, respectively. Clearance curves are similar between the two curves obtained from the internal carotid artery injection of $^{15}O_2$-hemoglobin ($^{15}O_2$–Hb) and ^{15}O-labeled water ($H_2^{15}O$). The clearance was faster for $C^{15}O$–hemoglobin ($C^{15}O$–Hb) injection. PET, positron emission tomography.

clearance slopes after 5 seconds of the peak consisted of the early (faster) and delayed (slower) components in all experiments with the $^{15}O_2$–Hb and the $H_2^{15}O$–saline injections. A sharp peak was visible after the $^{15}O_2$–Hb blood sample injection at the beginning, but this was not seen after $H_2^{15}O$ sample injection. It can also be seen that the clearance slopes were visually identical between the $^{15}O_2$–Hb and the $H_2^{15}O$–saline injections in both early (5 to 40 seconds) and late (70 to 240 seconds) phases. Results from the

Table 1. List of hemodynamic parameters and summary results of clearance slopes fitted the single exponential function to the first 5 to 40 seconds (early) and 80 to 240 seconds (late) phases after the peak of the clearance curves

	Weight (kg)	*Age (year)*	*Hb (g/dL)*	*Systolic/diastolic blood pressure (mm Hg)*	*Heart rate (bpm)*		*$PaCO_2$ (mm Hg)*	*Slope (minute) (early)*	*Slope (minute) (late)*
Monkey 1	7.5	3	13.5	110/60	136	$^{15}O_2$–Hb	42.1	0.372 ± 0.078	0.212 ± 0.070
						$H_2^{15}O$	42.5	0.374 ± 0.059	0.208 ± 0.052
Monkey 2a	7.1	4	12.6	115/65	133	$^{15}O_2$–Hb	42.6	0.468 ± 0.076	0.265 ± 0.070
						$H_2^{15}O$	43.4	0.513 ± 0.045	0.292 ± 0.014
Monkey 2b	7.1	4	12.9	132/90	131	$^{15}O_2$–Hb	39.2	0.452 ± 0.038	0.275 ± 0.017
						$H_2^{15}O$	40.6	0.475 ± 0.083	0.296 ± 0.014
Average	7.23	3.7	13.0	119/71.6	133.3	$^{15}O_2$–Hb	41.3	0.430 ± 0.076	0.251 ± 0.061
						$H_2^{15}O$	42.2	0.454 ± 0.085	0.265 ± 0.051

HB, hemoglobin; $H_2^{15}O$, ^{15}O-labeled water; $^{15}O_2$–Hb, $^{15}O_2$–hemoglobin; $PaCO_2$, partial pressures of carbon dioxide, ROI, region of interest. Clearance slope values are presented for mean and 1 s.d. for each experiment among five ROIs, and also for pooled data for five ROIs of total three experiments.

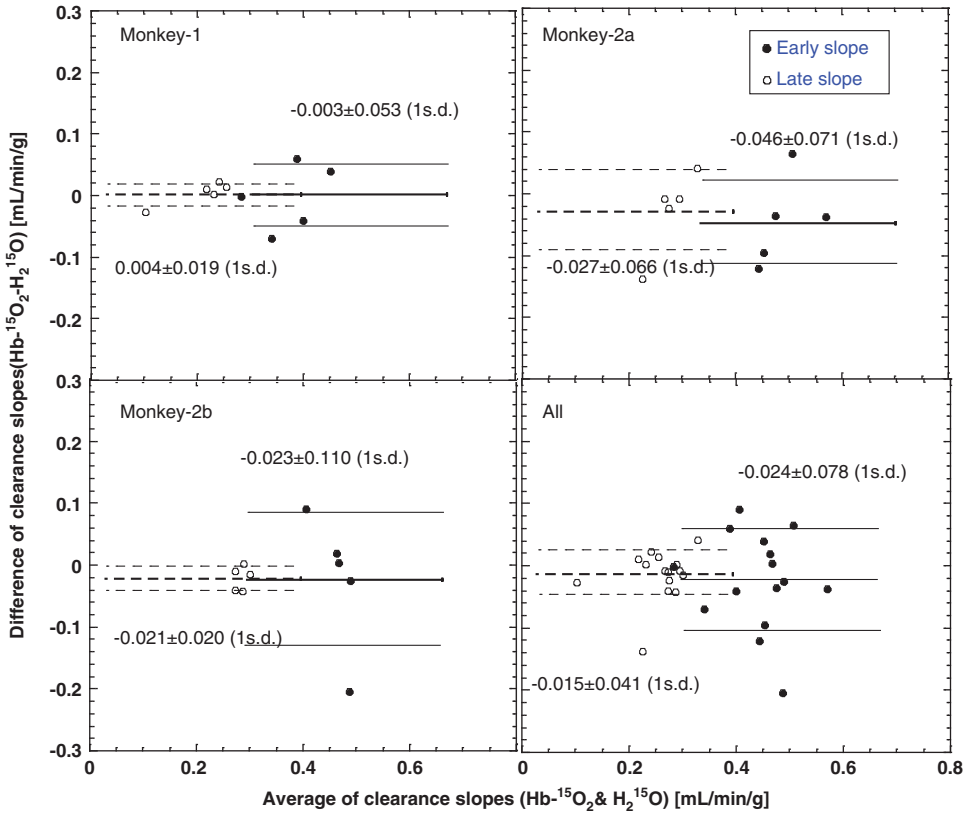

Figure 5. Results from the Bland–Altman plot analysis obtained from the single exponential fitting analysis for each of the three experiments, and for all pooled data (All). The agreement of the two assessments showed uncertainty of ~20% (1 s.d. of 0.078 and 0.041 at averaged slope value of ~0.4 and 0.2 corresponding to the faster and slower components, respectively) for each of the two components. $^{15}O_2$–Hb, $^{15}O_2$–hemoglobin; $H_2^{15}O$, ^{15}O-labeled water.

fitting of the clearance slopes for both the early (faster) and late (slower) slopes to the single exponential function are summarized in Table 1. Interslice variations of the slope values were 10% to 20% in each experiment, for both the early (fast) and the late (slower) slopes in the $^{15}O_2$–Hb and the $H_2^{15}O$–saline injections. Within these variations, no significant difference was detected between $^{15}O_2$–Hb and $H_2^{15}O$–saline injections in each of the three experiments for both the early (fast) and the late (slower) slopes. The residues of the fitting showed no significant correlation in relation to the time on the logarithmic domain, in the early and late phase slopes, both for the $^{15}O_2$–Hb and $H_2^{15}O$–saline injections in each of the three experiments.

Figure 5 shows the Bland–Altman's plots demonstrating the difference in the clearance slope values being not significantly different between the $^{15}O_2$–Hb and $H_2^{15}O$–saline injection both in the early (faster) and late (slower) phases, at each of the three experiments. One s.d. values of the differences were 0.078 minutes and 0.041 minutes, and the averaged values between the $^{15}O_2$–Hb and $H_2^{15}O$–saline injections 0.442 minutes and 0.258 minutes corresponding to the early (faster) and late (slower) slopes, respectively, resulting in the ratio of these values being 17.6% and 15.9% for the entire analysis.

DISCUSSION

The clearance slopes of ^{15}O-radioactivity following the slow bolus injection of $^{15}O_2$–Hb, $H_2^{15}O$–saline and $C^{15}O$–Hb into the ICA were determined for local cerebral regions using sequential PET

imaging in three independent experiments on two monkeys (*M. fascicularis*). The clearance curves consisted of faster (early) and slower (late) components after 4 seconds of the peak, corresponding to the gray matter and white matter tissues, respectively. The clearance curves were well reproduced by the single exponential functions for both the early (5 to 40 seconds) and late (80 to 240 seconds) periods, in which residuals showed no time dependency on the logarithmic domain in all fits. It should also be noted that the variation (1 s.d.) in the differences of the slope values showed no significant difference between the $^{15}O_2$–Hb and $H_2^{15}O$ injections was for both the gray matter and the white matter components in each experiment. Variation of the differences was 17.6% and 15.9% relative to the mean slope values in the entire analysis, corresponding to the faster and slower components, respectively. These variations were associated with the uncertainty of the PET assessment, and also attributed to the variation of true CBF values at different slice levels. The agreement of the slope values found in this study between the $^{15}O_2$–Hb and $H_2^{15}O$ injections supports the traditional hypothesis shown in Figure 1 on the $^{15}O_2$ kinetics in the cerebral tissue, namely the non-negligible amount of clearance from the brain in the form of $^{15}O_2$ to the capillary bed, and as well as the non-negligible amount of effective retention of $^{15}O_2$ molecule in the brain tissue.

Accuracy of the assessment is well supported in two-dimensional PET, by involving corrections for detector inhomogeneity, random coincidence, dead time, attenuation and scatter, and the well-established reconstruction procedures. Contamination of signals and hence, random coincidence events can be accurately corrected, and were only small in this study. The dead time count loss was only less than 5% at the peak of total counting rate of $\sim$60 kcps over the whole field of view. Use of an artificial lung[12] should have contributed to minimize the risk for the possible damage of the red cells and hemoglobin during the labeling procedures. The injected sample volumes of 0.4 mL into an over a 3 to 4 seconds period (namely 0.1 mL/second or 6 mL/minute) was smaller than the natural cerebral perfusion of $\sim$20 mL/minute, as estimated by assuming the averaged regional perfusion of 0.3 mL/minute per gram, and the whole brain weight of 60 g. Injection of the samples applied in this study thus unlikely causes disturbance in the cerebral circulation. It should also be noted that the contribution of recirculation of injected radioactivity can be considered only small, because only a small fraction of injected radioactivity can return the cerebral tissues. As the decrease of the brain radioactivity was only 2 to 3 times even at the end of the PET imaging, amount of the recirculating radioactivity should cause negligible effects. Despite the small number of the experiments, the results from this study suggest that the presence of significant difference in the clearance slopes between $^{15}O_2$–Hb and $H_2^{15}O$ injections would be unlikely. Most of the previous approaches[5–7,15–17] that quantitatively assessed $CMRO_2$ and CBF in various clinical settings, which stand for these assumptions, are thus considered to be adequate.

It has been believed that oxygen is excessively delivered into intact brain as compared with its utilization, resulting in significant amount of oxygen tension in the brain tissue[18]. This suggests that the back diffusion of radioactivity could exist in the form of $^{15}O_2$ from the tissue to the blood. However, the effective contribution of the back diffusion was not visible in the clearance slopes, namely no significant difference was seen in the slopes between the $^{15}O_2$–Hb and $H_2^{15}O$–saline injection in the present study. This is attributed to the short life time of oxygen molecule in the brain tissue associated with the high oxidative metabolism in the cerebral tissue. Our results are, however, controversial to those by Seki *et al*[10], who claimed faster clearance after $^{15}O_2$–Hb than $H_2^{15}O$–saline administration. Exact reasons are not known, but could be attributed to a couple of methodological factors such as: (a) the observed time–activity curves could have been contaminated with backgrounds from surroundings particularly at the beginning after the $^{15}O_2$–Hb, (b) small size of the animal relative to the injecting volume of 30 to 50 μL in 2 to 3 seconds, corresponding to the perfusion of 0.3 to 0.75 mL/minute per gram, equivalent to the whole brain circulation of this animal, and (c) possible damage of hemoglobin during the bubbling procedures, possibly causing unexpected behavior in the kinetics. Exact reason is not known, and further evaluation is warranted.

There are limitations in this study: (a) Only three independent experiments were carried out on two monkeys. Limited sample size is clearly the weakness of this study. This was simply due to the difficulty of having more animals for this experiment. Given the reproducibility being 17.6% and 15.9% among PET slices corresponding to the faster and slower clearance slopes, however, additional experiments on different animals likely cannot detect significant differences between the $^{15}O_2$–Hb and $H_2^{15}O$–saline injections, even if it exists. (b) Positron emission tomography scans were carried out only at the baseline condition during the anesthesia, but not during hyperemia or other stressed conditions. This was due to the need for minimizing the possible damage to the animals, as they were scheduled to participate in another study of evaluating the revascularization therapeutic trials after embolic stroke. Repeating the same set of experiments in the stressed conditions is more challenging to maintain the arterial partial pressure of carbon dioxide, the heart rate, and the blood pressure. We were also concerned that no reason is clearly shown why the clearance slope could be altered after the physiological stimulation. It would however be of an interest to confirm the identical slope values also after the physiological stress is involved, in the future. (c) Due to the limited spatial resolution of the PET device employed in this study ($\sim$10 mm full width at half maximum), there must be significant contribution of heterogeneity of CBF and $CMRO_2$ within a selected ROI. This includes not only the gray matter and white matter heterogeneity, which could be observed as faster and slower clearance slopes in this study, but also in homogeneous distribution in a small local area within the selected ROI. (d) The clearance slopes ranging from 0.37 to 0.45 minutes for the faster component was smaller than the clearance slope-based CBF values reported previously with PET involving the partial volume correction on monkeys[19]. This could be attributed to different anesthesia protocols. In this experiment, anesthesia was maintained under the continuous intravenous infusion of propofol, while in the earlier study, the anesthesia was maintained by repetitive intramuscular injections of a mixture of xylazin and ketamine. Kaisti *et al*, [20] demonstrated difference in the change of absolute CBF and $CMRO_2$ values in normal young adults dependent on the anesthesia. It was also demonstrated that both CBF and $CMRO_2$ can be reduced during the propofol administration, which might explain at least a part of the difference from the earlier publications. (e) There was significant amount of collateral circulation though the Willis Ring to the collateral hemisphere as can be seen in the accumulated images on Figure 3. With the same reason, injected ^{15}O-radioactivity should be smeared by the collateral circulation. This may cause systematic bias in the difference between the $^{15}O_2$–Hb and $H_2^{15}O$–saline experiments, although this contribution is likely small enough. (f) The initial peak observed after the administration of $^{15}O_2$–Hb but not after $H_2^{15}O$–saline sample was attributed to the vascular radioactivity, which was not extracted into the cerebral tissue. The first-pass extraction fraction assessment from this portion as proposed by Raichle *et al*[9] could not be applied due to the slow bolus administration in this study. Smaller amount blood samples needs to be prepared, but the need for a higher radioactivity concentration requires increased production of $^{15}O_2$ radioactivity in the cyclotron target. Our cyclotron has not been prepared for that amount of production. Shorter temporal resolution less than 1-second interval images are limited in the out PET reconstructed images. Further efforts are needed in order to assess the first-pass extraction fraction on local brain regions from the sequential PET images.

In conclusion, dynamic PET imaging was performed to investigate differences in the clearance rates of cerebral ^{15}O-radioactivity after bolus injections of $^{15}O_2$–Hb and $H_2^{15}O$ into the ICA. Analysis of the bi-exponential time–activity curves suggested that a significant difference between the rates is unlikely for both the early and late stage data. Even though the number of experiments should be increased to improve the statistics, the results imply that the mathematical model presented in Figure 1 is adequate for quantitative assessment of $CMRO_2$ and may encourage further development of PET protocols to improve performance and logistics.

DISCLOSURE/CONFLICT OF INTEREST

The authors declare no conflict of interest.

ACKNOWLEDGMENTS

The authors gratefully acknowledge the staff of Department of Investigative Radiology, National Cerebral and Cardiovascular Center, Osaka, Japan, particularly Drs Takuya Hayashi and Hiroshi Watabe with their technical assistance during the experiment.

REFERENCES

1 Frackowiak RS, Jones T, Lenzi GL, Heather JD. Regional cerebral oxygen utilization and blood flow in normal man using oxygen-15 and positron emission tomography. *Acta Neurol Scand* 1980; **62**: 336–344.
2 Frackowiak RS, Lenzi GL, Jones T, Heather JD. Quantitative measurement of regional cerebral blood flow and oxygen metabolism in man using ^{15}O and positron emission tomography: theory, procedure, and normal values. *J Comput Assist Tomogr* 1980; **4**: 727–736.
3 Subramanyam R, Alpert NM, Hoop B, Brownell GL, Taveras JM. Model for regional cerebral oxygen distribution during continuous inhalation of O-15(2), Co-O-15, and Co2-O-15. *J Nucl Med* 1978; **19**: 48–53.
4 Hattori N, Bergsneider M, Wu HM, Glenn TC, Vespa PM, Hovda DA *et al.* Accuracy of a method using short inhalation of (15)O-O(2) for measuring cerebral oxygen extraction fraction with PET in healthy humans. *J Nucl Med* 2004; **45**: 765–770.
5 Ohta S, Meyer E, Fujita H, Reutens DC, Evans A, Gjedde A. Cerebral [^{15}O]water clearance in humans determined by PET: I. Theory and normal values. *J Cereb Blood Flow Metab* 1996; **16**: 765–780.
6 Kudomi N, Hayashi T, Teramoto N, Watabe H, Kawachi N, Ohta Y *et al.* Rapid quantitative measurement of $CMRO_2$ and CBF by dual administration of ^{15}O-labeled oxygen and water during a single PET scan-a validation study and error analysis in anesthetized monkeys. *J Cereb Blood Flow Metab* 2005; **25**: 1209–1224.
7 Kudomi N, Hirano Y, Koshino K, Hayashi T, Watabe H, Fukushima K *et al.* Rapid quantitative CBF and CMRO(2) measurements from a single PET scan with sequential administration of dual (15)O-labeled tracers. *J Cereb Blood Flow Metab* 2013; **33**: 440–448.
8 Ter-Pogossian MM, Eichling JO, Davis DO, Welch MJ. The measure *in vivo* of regional cerebral oxygen utilization by means of oxyhemoglobin labeled with radioactive oxygen-15. *J Clin Invest* 1970; **49**: 381–391.
9 Raichle ME, Grubb RL, Eichling JO, Terpogossian MM. Measurement of brain oxygen utilization with radioactive oxygen-15 - experimental verification. *J Appl Physiol* 1976; **40**: 638–640.
10 Seki C, Kershaw J, Toussaint PJ, Kashikura K, Matsuura T, Fujita H *et al.* O-15 radioactivity clearance is faster after intracarotid bolus injection of O-15-labeled oxyhemoglobin than after O-15-water injection. *J Cereb Blood Flow Metab* 2003; **23**: 838–844.
11 Kudomi N, Hayashi T, Watabe H, Teramoto N, Piao R, Ose T *et al.* A physiologic model for recirculation water correction in $CMRO_2$ assessment with $^{15}O_2$ inhalation PET. *J Cereb Blood Flow Metab* 2009; **29**: 355–364.
12 Magata Y, Temma T, Iida H, Ogawa M, Mukai T, Iida Y *et al.* Development of injectable O-15 oxygen and estimation of rat OEF. *J Cereb Blood Flow Metab* 2003; **23**: 671–676.
13 Kudomi N, Choi E, Yamamoto S, Watabe H, Kim K, Shidahara M *et al.* Development of a GSO detector assembly for a continuous blood sampling system. *IEEE Trans Nucl Sci* 2003; **50**: 70–73.
14 Clarke J, Tochon-Danguy HJ. "R2D2'' a bedside [oxygen-15] water infuser. In: Weinrich R (ed) *The 6th International Workshop on Targetry and Target*. PSI: Villigen, Switzerland, 1991.
15 Lammertsma AA, Jones T, Frackowiak RS, Lenzi GL. A theoretical study of the steady-state model for measuring regional cerebral blood flow and oxygen utilisation using oxygen-15. *J Comput Assist Tomogr* 1981; **5**: 544–550.
16 Mintun MA, Raichle ME, Martin WR, Herscovitch P. Brain oxygen utilization measured with O-15 radiotracers and positron emission tomography. *J Nucl Med* 1984; **25**: 177–187.
17 Iida H, Jones T, Miura S. Modeling approach to eliminate the need to separate arterial plasma in oxygen-15 inhalation positron emission tomography. *J Nucl Med* 1993; **34**: 1333–1340.
18 Mintun MA, Lundstrom BN, Snyder AZ, Vlassenko AG, Shulman GL, Raichle ME. Blood flow and oxygen delivery to human brain during functional activity: theoretical modeling and experimental data. *Proc Natl Acad Sci USA* 2001; **98**: 6859–6864.
19 Iida H, Law I, Pakkenberg B, Krarup-Hansen A, Eberl S, Holm S *et al.* Quantitation of regional cerebral blood flow corrected for partial volume effect using O-15 water and PET: I. Theory, error analysis, and stereologic comparison. *J Cereb Blood Flow Metab* 2000; **20**: 1237–1251.
20 Kaisti KK, Langsjo JW, Aalto S, Oikonen V, Sipila H, Teras M *et al.* Effects of sevoflurane, propofol, and adjunct nitrous oxide on regional cerebral blood flow, oxygen consumption, and blood volume in humans. *Anesthesiology* 2003; **99**: 603–613.